Leppäkoski, H., Collin, J. & Takala, J.
Journal of Signal Processing Systems (2013) 71: 287.
doi:10.1007/s11265-012-0711-5

Pedestrian Navigation Based on Inertial Sensors, Indoor Map, and WLAN Signals

H. Leppäkoski, J. Collin, and J. Takala
Department of Computer Systems,
Tampere University of Technology, Tampere, Finland

October 19, 2012

Abstract

As satellite signals, e.g. GPS, are severely degraded indoors or not available at all, other methods are needed for indoor positioning. In this paper, we propose methods for combining information from inertial sensors, indoor map, and WLAN signals for pedestrian indoor navigation. We present results of field tests where complementary extended Kalman filter was used to fuse together WLAN signal strengths and signals of an inertial sensor unit including one gyro and three-axis accelerometer. A particle filter was used to combine the inertial data with map information. The results show that both the map information and WLAN signals can be used to improve the pedestrian dead reckoning estimate based on inertial sensors. The results with different combinations of the available sensor information are compared.

1 Introduction

While GPS provides pedestrian positioning solution for outdoor environments, the optimal strategy for pedestrian indoor positioning is still an open issue, as the indoor environment severely degrades the accuracy of satellite positioning or makes it totally impossible. Several information sources alternative to GPS have been proposed for pedestrian indoor positioning. MEMS sensors have been used to obtain dead reckoning estimate of the position. This estimate is based on previous known position, the distance traveled and direction of travel [2, 3, 4, 5]. Relatively short range radio communication signals, such as WLAN or Bluetooth signals have been used to obtain indoor position estimates [6, 7, 8]. The use of map information is common practice in car navigation [9], and similar principles have also been proposed for indoor positioning [10, 11, 12, 13].

All the mentioned approaches for indoor positioning have their strengths and weaknesses, and often a weakness of one system is the strength of another, so that the combination of several sources brings better performance than a

single source alone. To combine information from several sources, a suitable data fusion algorithm is needed.

In this paper, we propose the use of pedestrian dead reckoning (PDR) based on Microelectromechanical systems (MEMS) sensors fused together with WLAN based positioning, indoor map information, or both for indoor positioning. The sensor unit includes a heading gyro and a 3D-accelerometer. For the data fusion we propose two nonlinear Bayesian filters: for the fusion of PDR with WLAN positioning we propose Complementary Extended Kalman Filter (CEKF), and for the fusion of map information with other measurements, we propose a particle filter which uses state propagation principle similar to the CEKF. We also show that the processing load of the map information can be reduced by an appropriate prior sectioning of the map area so that only part of the obstacles need to be checked by the algorithm. The preliminary results of our tests have been reported in [1].

In the following sections we describe the models and algorithms and give positioning results based on real data from a pedestrian test walk.

2 Related Work

Kalman Filter (KF) is a common method for fusing together measurement information from various sources. When the measurement or propagation models or both include nonlinearities, Extend Kalman Filter (EKF) can be applied [14]. KF or EKF in complementary filter configuration is a common method to fuse redundant information from diverse types of sensors [14, 15]. Among others, complementary KF (CKF) or complementary EKF (CEKF) is applied for combining inertial sensors or DR systems with GPS and other aiding sensors in various navigation applications [15, 16, 17], and it can also be found in pedestrian navigation systems [18, 19]. From the references it can be noticed that the authors do not always mention that their filter is a complementary filter; however, the complementary filter structure of the CKF or CEKF can be identified based on the way how the filter states and its measurement inputs are chosen.

In CKF and CEKF, less signals are connected to measurement inputs of the filter than there are measurement signals available. In some complementary filter configurations, measurement inputs of the filter are differences of two measurement signals [15, 14]. In so called Embedded Reference Trajectory (ERT) configuration, some of the measurement signals are connected to the filter as deterministic inputs [15, 16, 20]. Therefore, CKF and CEKF require redundant measurement information. Background and overview on complementary filtering can be found in [14, 15], the latter of which also introduces the complementary filtering for nonlinear systems, i.e. CEKF. The ideas of [14, 15] are summarized and applied to a simple simulation example in [20].

The utilization of an indoor map for pedestrian navigation differs from the way the street maps are used in car navigation. In car navigation, the roads represent the possible locations of the car, and the task of the positioning algo-

rithm is to use some clever method to force the position estimate to the most probable road segment [9]. In indoor navigation, instead of defining possible routes the indoor map gives information about impossible locations and movements: the positioning algorithm uses information about walls and obstacles that the pedestrian is not able walk though [10, 11, 12, 13]. These are presented by line segments defined by the coordinates of their starting and ending nodes.

The map information about the walls and obstacles is difficult to formulate so that it could be applied with EKF. In particle filters, this kind of information can be taken into account easily: after each propagation step the algorithm can check whether the particles ended into obstacles or out of the room through the walls. If they did, their weight can be set to zero so that in the next resampling they will not survive. Background and overview on particle filtering can be found e.g. in [21].

In this paper, we propose two new algorithms, demonstrate their operation and make comparisons between them using results based on real data from a filed test. We propose a CEKF in ERT configuration for fusing PDR and WLAN positioning estimates; in our CEKF configuration the filter uses heading change and step length estimates produced by the PDR processing to propagate the state of the filter while the WLAN based position estimates are used as measurement updates of the filter. Unlike any of the CKF or CEKF systems described in [14, 15, 16, 17, 18, 20], our CEKF uses WLAN positioning as one information source. Our results also differ from results given [18], which also deals with PDR measurements, in that our filter is in ERT mode. In [16, 20], which present CKFs in ERT mode, the results are based on simulations while our results are based on field test measurements. In [19], where also both WLAN and PDR were used in CEKF ERT configuration, the PDR hardware was shoe mounted while in our system it was attached to belt. The shoe mounted PDR system is generally more accurate as it allows the use of zero-velocity updates [22]. However, in practical applications it has some disadvantages, e.g., due to its position it is vulnerable to knocks and it is difficult be protected unless it is not embedded into the the structure of the shoe, in which case the power supply and maintenance of the unit comes difficult.

For utilizing indoor map information about obstacles we propose a bootstrap particle filter [21] where the particles are propagated using the same ERT principle as in the CEKF, i.e., the propagation of particle states utilizes estimates provided by the PDR computations and either the WLAN based position estimates or the map information or both are used to compute the particle weights. Particle filters and map information have been used in [10, 12]; our system differs from these in that our system includes also DR sensor unit to determine the distance traveled and heading. The system in [11] includes also accelerometer to determine the distance traveled but does not include sensor to measure heading like our system. As in this paper, the authors of [11] also give comparison results that are based on different combinations of the available information sources and algorithms processing the data from the same field tests. In [13] also gyros are included to enable the heading estimation; this system differs from ours in that it uses a shoe mounted PDR unit while the PDR unit

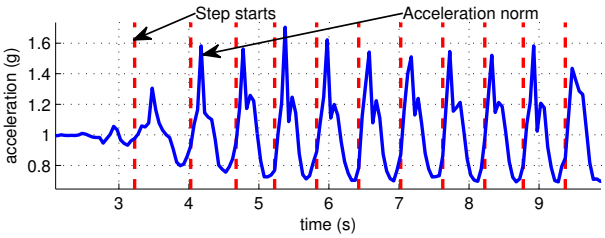

(a) Step detection based on acceleration norm.

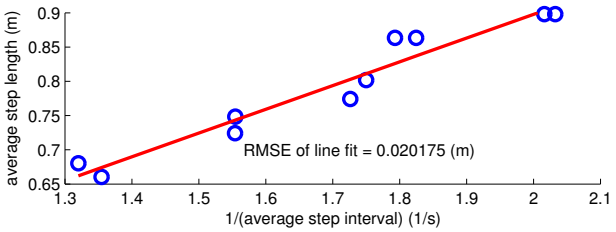

(b) Step length calibration using test data sets. Observations shown with circles.

Figure 1: Estimation of travelled distance

in our system is attached to belt of the pedestrian.

In many reports that consider indoor positioning, the field tests have been conducted in office environments consisting of corridors and rooms. We present results of field test conducted in a university library, where radio signal propagation pattern is different; there are few walls that totally block the signals while at the same time there are lot of obstacles that distort the signal propagation causing either non-line-of-sight conditions or strong signal attenuation. However, these obstacles provide lot of map information for data fusion algorithm.

3 Information sources

In this section, the processing for pedestrian dead reckoning, usage of map information, and positioning based on WLAN signals are described.

3.1 Pedestrian dead reckoning

The length of the distance traveled can be obtained by performing double integration of an accelerometer signal. Unfortunately, this approach suffers from unbound error growth due to, e.g., tilt errors of the sensor unit. In pedestrian navigation such errors can be avoided by using step detection algorithm and step length estimation based on accelerometer signal pattern [3, 4, 23].

To avoid the effect of the sensor unit tilt in the acceleration signal, we use

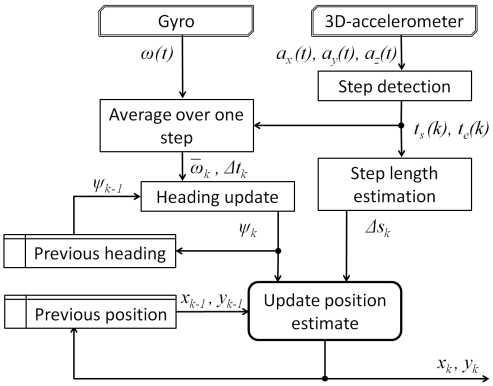

Figure 2: PDR algorithm based on heading gyro and 3D-acceleration measurements.

the norm of the measured acceleration for step detection and step length estimation since the norm is insensitive to the orientation of the sensor unit. The procedure for step detection consists of the following steps: (1) Low pass filtering and resampling of the signal to the frequency of 20-50 Hz, (2) Computation of the norm of acceleration components, i.e. $a(t) = \sqrt{a_x(t) + a_y(t) + a_z(t)}$, (3) Detection of a step start when the acceleration norm crosses g (gravitational acceleration) so that it is followed by rise rate and peak height that exceed the preset limits, (4) Detection of a step end at the start of the next step or 0.9 s after the previous step start, which ever happens earlier. The use of acceleration norm for step detection is illustrated in Fig. 1(a).

To obtain the calibration parameters for presenting the step length as a function of step frequency [2], ten sets of walking data were collected in a straight corridor using an accelerometer triad. The straight leg of a known length was walked ten times. To obtain step samples with different step lengths, the walker tried to adjust the walking speed to normal, slower than normal, slow, faster than normal, and fast, as it is known that the step length is also a function of the walking speed [2]. With the data, the steps were detected from the acceleration norms and step intervals were determined. Using step intervals averaged over each walk, the number of detected steps per walk, and the known length of total traveled distance per walk, a linear fit can be found between average step frequencies and step lengths of each test data set, as shown in Fig. 1(b).

The sensor based PDR estimate is computed by starting from initial coordinates, x_0, y_0, and initial heading angle ψ_0. The heading and horizontal coordinates are propagated by

$$\begin{bmatrix} \psi_k \\ x_k \\ y_k \end{bmatrix} = \begin{bmatrix} \psi_{k-1} + \bar{\omega}_k \Delta t_k \\ x_{k-1} + \Delta s_k \cos\psi_k \\ y_{k-1} + \Delta s_k \sin\psi_k \end{bmatrix}, \tag{1}$$

where Δs_k is the distance traveled on the step with index k and Δt_k is the

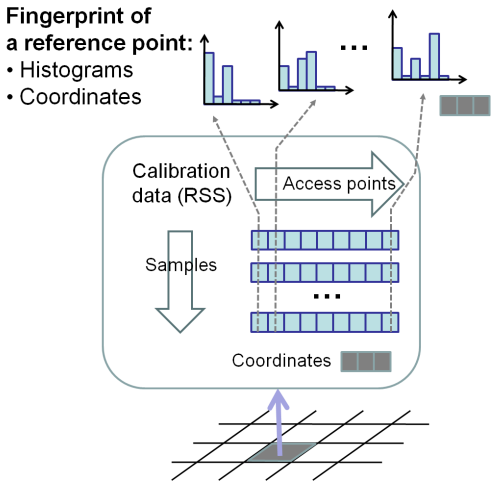

Figure 3: WLAN radio map with histograms.

length of the sample interval, which in this case is the same as the step interval; Δt_k varies according to the walking style and speed of the pedestrian. $\bar{\omega}_k$ is the average angular rate measurement by the gyro, averaged over the step interval Δt_k. The block diagram of the PDR computations is shown in Fig. 2.

3.2 Indoor map

In indoor navigation, the positioning algorithm uses information about walls and obstacles that the pedestrian is not able walk though. These are presented by line segments defined by the coordinates of their starting and ending nodes. In particle filter implementation, the algorithm checks for each particle transition whether the transition line intersects any of the obstacle lines. The computational load of this process is significant if the number of obstacle lines is large. However, the number of line crossing checks can be reduced, if the obstacle lines close to each other are grouped. Then, instead of checking crossings with all the possible line segments, the algorithm first searches the line groups in whose area the particle transition happens, and checks the line crossings only with the lines segments of these groups.

3.3 WLAN positioning

WLAN signals can be used in several ways to estimate position. In this paper, we use WLAN fingerprinting [6, 24], where experimentally defined radio map is generated offline to locally model the relation between the user position and Received Signal Strengths (RSS) of the WLAN signals received by the user device. The implemented probabilistic estimation algorithm uses WLAN fingerprints which include histogram approximations of Probability Density Functions

(PDF) of the WLAN RSS [24]. For the radio map, reference points are spread over the area to be mapped. The RSS conditions in each reference point are described by the PDFs of the RSS separately for each available access point (AP). The PDFs are approximated by histograms as described in Fig. 3.

In histogram approximation of PDF, the RSS range is divided into n_B bins; the fine-resolution scale becomes discrete scale with coarse resolution. A histogram based radio map stores marginal distributions $p(y|\ell)$ for each reference point location ℓ, , i.e. the conditional probabilities that the measured RSS vector y can be observed at location ℓ. In estimation phase, the conditional probabilities are employed to calculate the posterior probability $p(\ell|y)$, i.e. the probability of being located at ℓ, given the measured RSS values y.

The posterior probabilities of the locations are computed using Bayes' Theorem [25] :

$$\begin{aligned} p(\ell|y) &= \frac{p(y|\ell)\, p(\ell)}{p(y)} \\ &= \frac{p(y|\ell)\, p(\ell)}{\sum_{\ell' \in L} p(y|\ell') p(\ell')} , \end{aligned} \tag{2}$$

where $p(\ell)$ is the prior probability of being at location ℓ. In this algorithm, we use a non-informative uniform distribution, i.e. $p(\ell)$ is equal for each ℓ. The set L contains all the possible reference locations and $p(y)$ is the probability of the measurement vector $y = [y_1, \cdots, y_{n_{AP}}]$ over all locations. n_{AP} is the number of access points. $p(y)$ does not depend on location and is treated as a normalizing constant. The estimate

$$\hat{\ell} = E(\ell|y) = \sum_{\ell' \in L} \ell' p(\ell'|y) \tag{3}$$

minimizes the expected squared location error [25]. Assuming equal $p(\ell)$ for all ℓ and independence of observations y_i, the posterior probabilities $p(\ell|y)$ in (3) can be computed using Bayes' theorem:

$$p(\ell|y) = \frac{\prod_{i=1}^{n_{AP}} p(y_i|\ell)}{\sum_{\ell' \in L} (\prod_{i=1}^{n_{AP}} p(y_i|\ell'))}. \tag{4}$$

4 Proposed algorithms and models

In this section the algorithms and models used in CEKF and particle filter implementations are described.

4.1 Complementary Extended Kalman Filter

A simple process model with errors modeled as white noises is applied, which does not require special error states. The elements of the state vector $\mathbf{x}_k$ are the following: x_{1_k} = heading, x_{2_k} = x-coordinate, and x_{3_k} = y-coordinate, and therefore the state propagation resembles the dead reckoning presented in (1).

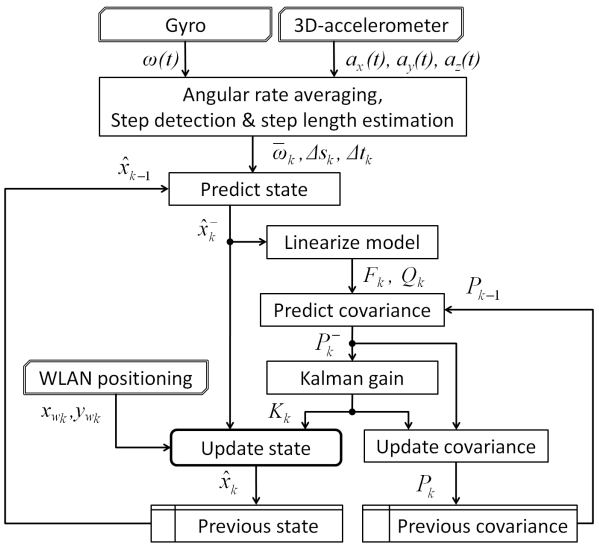

Figure 4: CEKF algorithm for fusing the measurements of heading gyro and 3D-accelerometer together with WLAN based position estimates.

The filter is started from initial estimate $\hat{\mathbf{x}}_0$ and initial covariance $\mathbf{P}_0$, which are set according to the best available estimate about the initial position and the uncertainty of the initial position information. The block diagram of the CEKF algorithm is shown Fig. 4.

The state is propagated by using

$$\hat{\mathbf{x}}_k^- = \hat{\mathbf{x}}_{k-1} + \begin{bmatrix} \bar{\omega}_k \Delta t_k \\ \Delta s_k \cos \hat{x}_{1_{k-1}} \\ \Delta s_k \sin \hat{x}_{1_{k-1}} \end{bmatrix}, \tag{5}$$

where $\hat{\mathbf{x}}_{k-1}$ denotes the posterior estimate after the measurement update using the $(k-1)$th measurement samples, while $\hat{\mathbf{x}}_k^-$ is the prior estimate for kth time step. The definitions of $\bar{\omega}_k$, Δs_k, and Δt_k are the same as in (1) and $\hat{x}_{1_{k-1}}$ is the previous posterior estimate of heading. The state matrix $\mathbf{F}_k$, needed for covariance propagation, is obtained by taking the partial derivative of (5):

$$\mathbf{F}_k = \begin{bmatrix} 1 & 0 & 0 \\ -\Delta s_k \sin \hat{x}_{1_k}^- & 1 & 0 \\ \Delta s_k \cos \hat{x}_{1_k}^- & 0 & 1 \end{bmatrix}. \tag{6}$$

As the effect of the step length uncertainty is multiplied by sin and cos functions of the heading, the state noise $\mathbf{Q}_k$ is also approximated on every propagation step:

$$\mathbf{Q}_k = diag\left(\begin{bmatrix} V_\omega \\ \cos^2\left(\hat{x}_{1_k}^-\right) V_{\Delta s} \\ \sin^2\left(\hat{x}_{1_k}^-\right) V_{\Delta s} \end{bmatrix} \right), \tag{7}$$

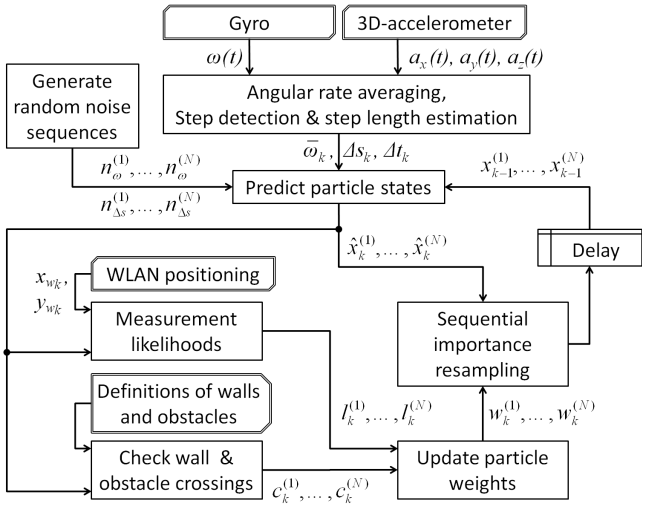

Figure 5: Particle filter algorithm for fusing the measurements of heading gyro and 3D-accelerometer together with WLAN based position estimates and map information.

where V_ω is the variance of angular rate measurement and $V_{\Delta s}$ is the variance of step length estimate. The covariance propagation to obtain the prior covariance $\mathbf{P}_k^-$ is now

$$\mathbf{P}_k^- = \mathbf{F}_k \mathbf{P}_{k-1} \mathbf{F}_k^T + \mathbf{Q}_k, \tag{8}$$

where $\mathbf{P}_{k-1}$ is the posterior covariance from the previous time step. The measurement input of the filter is $\mathbf{z}_k = [x_{W_k}\ y_{W_k}]^T$, consisting of the x and y coordinates estimated using WLAN fingerprints, and measurement matrix is

$$\mathbf{H} = \begin{bmatrix} 0 & 1 & 0 \\ 0 & 0 & 1 \end{bmatrix}.$$

Now the equations for measurement update of state $\hat{\mathbf{x}}_k$ and covariance $\mathbf{P}_k$ are

$$\begin{aligned} \mathbf{K}_k &= \mathbf{P}_k^- \mathbf{H}^T \left(\mathbf{H} \mathbf{P}_k^- \mathbf{H}^T + \mathbf{R} \right)^{-1} \\ \hat{\mathbf{x}}_k &= \hat{\mathbf{x}}_k^- + \mathbf{K}_k \left(\mathbf{z}_k - \mathbf{H} \hat{\mathbf{x}}_k^- \right) \\ \mathbf{P}_k &= \left(\mathbf{I}_{3x3} - \mathbf{K}_k \mathbf{H} \right) \mathbf{P}_k^-, \end{aligned} \tag{9}$$

where $\mathbf{R}$ is the covariance of WLAN based coordinate estimates and $\mathbf{I}_{3x3}$ is identity matrix.

4.2 Particle Filter

In this paper, we propose a bootstrap particle filter [21] where the particles are propagated using an equation similar to (5) used in CEKF, except that now the noise components of angular rate measurement and step length estimate

are simulated using a random number generator and then added to the particle states:

$$\hat{\mathbf{x}}_k^{(i)} = \hat{\mathbf{x}}_{k-1}^{(i)} + \begin{bmatrix} \left(\bar{\omega}_k + n_\omega^{(i)}\right) \Delta t_k \\ \left(\Delta s_k + n_{\Delta s}^{(i)}\right) \cos \hat{x}_{1_{k-1}} \\ \left(\Delta s_k + n_{\Delta s}^{(i)}\right) \sin \hat{x}_{1_{k-1}} \end{bmatrix}. \tag{10}$$

Here (i) is the index of the particle. The noise components $n_\omega^{(i)}$ and $n_{\Delta s}^{(i)}$ are generated so that their variances are the same as the variance values of angular rate and step length that were used in CEKF.

The evaluation of the likelihoods of the particle positions is based on the same measurement variances for WLAN based x and y coordinate estimates that were used in CEFK. For each particle, the algorithm computes the likelihood of getting the position estimates $\mathbf{z}_k = [x_{W_k}\ y_{W_k}]^T$ from WLAN positioning. The zero-mean Gaussian distribution is assumed for errors of $\mathbf{z}_k$. After a measurement update from WLAN positioning, the weights of the particles are obtained from the measurement likelihoods normalized by their sum.

The weight update with indoor map information is performed every time the algorithm has propagated particles using the PDR information. If the obstacle line check reveals that the last particle transition has crossed an obstacle line, the weight of the particle is set to zero, otherwise it is not changed. Before the next particle state propagation, importance resampling is performed, i.e., the particle cloud is resampled so that the probability of a particle to continue to next propagation step is proportional to the weight of the particle. In this phase, the particles that crossed obstacle lines will disappear from the particle cloud, as their weights are zero. The block diagram of the particle filter algorithm is shown Fig. 5.

5 Field tests and results

A test walk was conducted in the library of the Tampere University of Technology. The test route consisted of four loops in the library and it took 17 min to walk it. In the library only the outer walls totally block radio signals, but there are lot of book shelves that cause either strong attenuation or non-line-of-sight conditions for the radio signal propagation. On the other hand, as the book shelves are obstacles that the pedestrian cannot walk though they provide useful map information for the particle filter. In this section, the results of positioning tests are described. With the same data, we also tested obstacle line groupings with different widths of cells in map grid to find the line grouping that minimizes the run time of the particle filter processing.

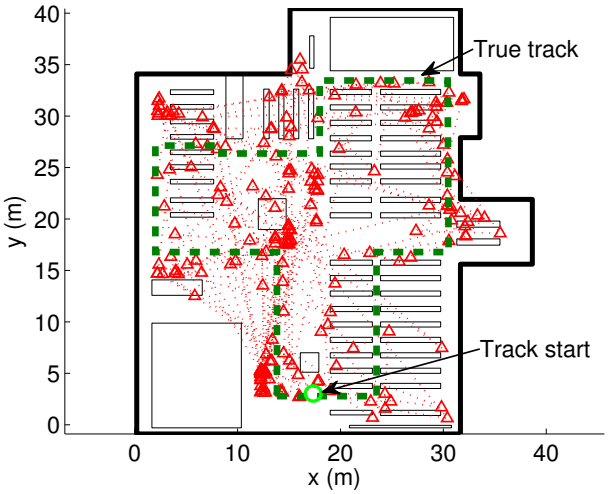

Figure 6: WLAN based position estimates shown with triangles. Transitions between consecutive estimates shown with narrow dotted lines.

5.1 WLAN only

The WLAN signal strengths were collected using a mobile handset, which outputs WLAN scan results at 2.3 s intervals. The position estimates computed from WLAN signal strengths that were collected along the test walk are shown in Fig. 6. From the figure we can see that the estimates are not evenly spread along the route, but rather concentrated in the center of the library area. The average position error is about 12 m.

5.2 PDR only

The inertial sensor unit used in pedestrian navigation test was a MEMS based sensor described in [26]. It includes an accelerometer triad and one gyro. In the test, the sensor unit was attached to the back of the test walker and aligned so that the sensitive axis of the gyro was vertical, i.e., it was able to measure heading changes.

The result of the unaided PDR estimate is shown in Fig. 7. It can be seen that during the first loop the traveled distance gets longer and the heading starts to get distorted. After the first loop, the three following loops seem to be quite similar in size and orientation. The maximum errors are 5 m in distance and 24° in heading angle.

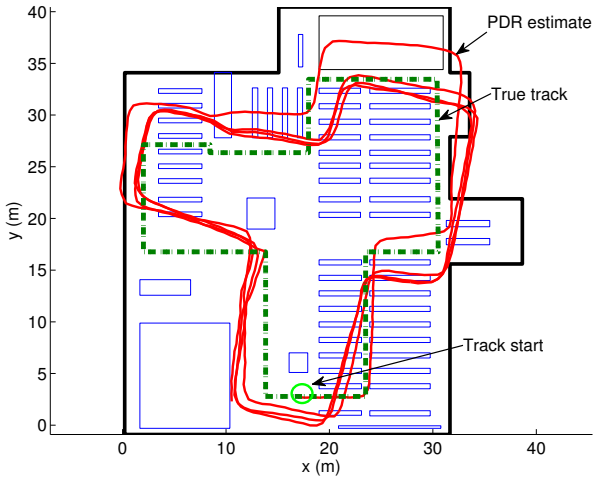

Figure 7: Unaided pedestrian dead reckoning.

5.3 Tuning of the filters

The CEKF and the particle filter were tuned by adjusting the covariance parameters V_ω, $V_{\Delta s}$, and $\mathbf{R}$. In the tests, the value of V_ω was $(0.2\,^\circ)^2$; it was chosen to be large enough to count for possible tilt errors of heading gyro during the walk. The step length uncertainty $V_{\Delta s}$ was $(0.4\,\mathrm{m})^2$. Its value was determined using the RMS estimation error given in Fig.1; if the RMSE is 0.0202 m over 10 walks with 39 steps on average, then the RMS uncertainty of one step is 0.4 m. The RMS uncertainty of WLAN based estimates of position coordinates was visually determined from Fig.6 to be 10 m, therefore diagonal elements of $\mathbf{R}$ were set to $(10\,\mathrm{m})^2$.

5.4 CEKF

The result of CEKF processing of the PDR and WLAN based position estimates is shown in Fig. 8. The CEKF was initialized with the same initial heading and coordinates as the unaided PDR estimate. It can be seen that CEKF can correct some of the skewness in PDR loops. The maximum errors can be estimated as 4 m in distance and 16° in heading.

5.5 Particle filters

In the first particle filter test, the filter was used to fuse PDR and map information, while in the second test, it was used to fuse also WLAN estimates with PDR and map information. The number of particles used in the tests was 500. The particle states were initialized with the same initial values as the CEKF.

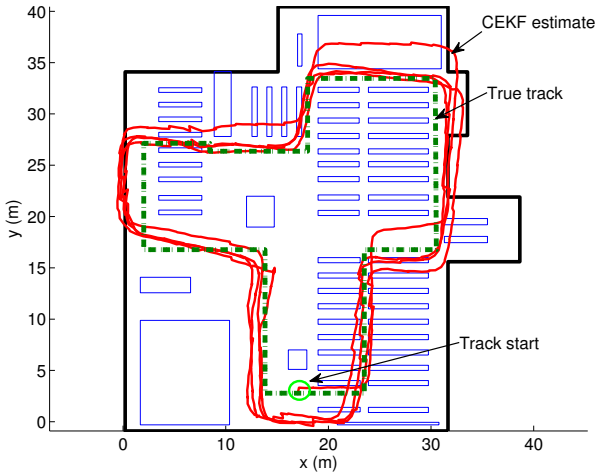

Figure 8: Complementary EKF using PDR and WLAN data.

The results of the tests are shown in Figures 9 and 10. The plotted particle filter track is the Minimum Mean Square Estimate (MMSE) computed from particle positions at each sampling instance. The maximum errors estimated are less than 3 m in distance and 12° in heading for both particle filters. However, the estimated track in Fig. 10 seems to follow the true track better than the track in Fig. 9, especially in upper and lower edges of the route. The reason for this can be seen in Fig. 6: there are many correct WLAN based position estimates available just before entering to these route segments, and therefore the WLAN estimates are able to improve the result.

5.6 Optimization of obstacle line grouping

To find the optimal grouping for obstacle lines, described in 3.2, the groupings were formed using square-shaped cells with cell widths from 2 to 41 m, growing in 1 m steps. With each grouping based on different cell width, the particle filter using PDR, WLAN and map information was run in Matlab to process all the measurement data. The run time of the computations were recorded, and the results are shown in Fig. 11. Based on the results we can conclude that the map data processing is the fastest when the cell width is 14 m. The grouping of map data clearly brings benefits: the run time without grouping, i.e., when all the obstacle lines belong to the same group with the cell width 41 m, is more than 400 s, while with optimal grouping the run time is only 150 s.

For comparison, the computation times of other methods presented in this paper are listed here: position computation using WLAN data only takes 1 s, computations for step detection, step length estimation, and the averaging of angular rate over one detected step takes about 15 s, DR processing from step

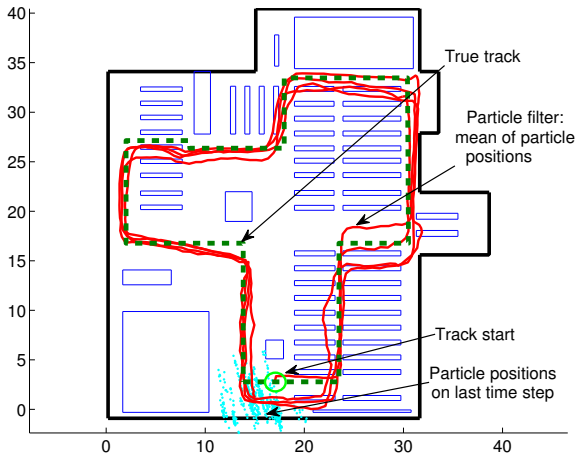

Figure 9: Particle filter using PDR data and map information.

lengths and delta headings takes less than 0.001 s, and CEKF processing from from step lengths, delta headings, and WLAN based positions takes about 0.2 s. The particle filter run times given in Fig. 11 do not include the run times of the necessary preprocessing phases, i.e., step detection, step length estimation, angular rate averaging, and WLAN positioning.

5.7 Comparison with related work

In [19], the RMS position error of the integrated IMU and WLAN positioning was 1.65 m and after initialization, the maximum error was about 4 m. In the setup of [19] the RMS position error using only WLAN fingerprinting was 3.18 m and maximum error 9 m, which is better than the maximum error of 12 m with our system. However, the maximum error 4 m of our CEKF, the integrated PDR and WLAN, is comparable with [19] despite the lack of zero velocity updates in our system. On the other hand, our system reached the 5 m maximum error with PDR only, which explains the improvement by the integration.

In [11], the mean error obtained using a particle filter, WLAN, map information and accelerometer was 4.3 m. In our system, the maximum error 3 m was better than this and can be obtained even without WLAN. This emphasizes the benefit of a sensor providing heading information in an indoor positioning system.

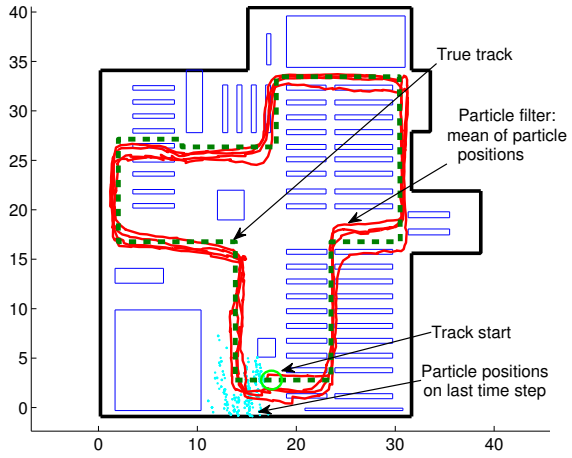

Figure 10: Particle filter using PDR and WLAN data and map information.

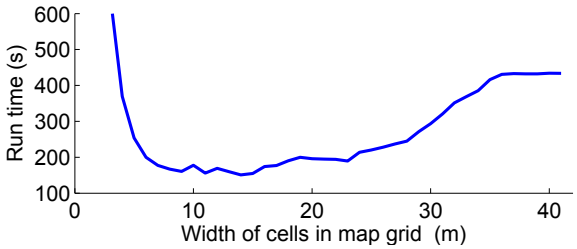

Figure 11: Run time of the particle filter processing as a function of the width of the cells in map grid.

6 Conclusions

In this paper, we proposed methods for combining information from inertial sensors, indoor map, and WLAN signals for pedestrian indoor navigation, and presented field test results obtained using the proposed algorithms. For the fusion of the PDR with WLAN positioning we proposed complementary Extended Kalman Filter and for fusion of the map information with other measurements we proposed a particle filter.

The inertial sensor unit used in these tests performed relatively well even as an unaided PDR system. However, fusing it with either WLAN positioning or map information improves accuracy. The quality of the WLAN position data is quite poor. Still the WLAN based position estimate includes some useful information to the data fusion filter. The WLAN based positioning is also complementary with map information: map information is relatively useless in open areas, where walls and obstacles cannot guide the particles, while in areas

with high density of obstacles this information is frequently available. Just the opposite, in areas dense with obstacles there is lot of disturbances present in WLAN signals which distort even a positioning algorithm using fingerprints, while in open areas the quality of WLAN based position estimate is better. However, due to the special characteristics of test area, it is difficult to generalize the results of our system directly to other types of environments without new field tests.

We also showed that the processing load of the map information can be reduced by an appropriate prior sectioning of the map area so that only part of the obstacles need to be checked by the algorithm. However, the optimal grouping very likely depends on the characteristics of the map area, i.e., the density and distribution of the obstacles, and therefore the need for an easily generalizable procedure for the grouping need to be studied.

References

[1] H. Leppäkoski, J. Collin, and J. Takala, "Pedestrian Navigation Based on Inertial Sensors, Indoor Map, and WLAN Signals," in *Proc. ICASSP 2012*, Kyoto, Japan, March 25–30 2012, pp. 1569–1572.

[2] R. W. Levi and T. Judd, "Dead reckoning navigational system using accelerometer to measure foot impacts," United States Patent No. 5,583,776, 1996.

[3] T. Judd, "A Personal Dead Reckoning Module," in *Proc. ION GPS 97*, Kansas City, MO, USA, Sept. 16–19 1997, pp. 47–51.

[4] Q. Ladetto, "On foot navigation : continuous step calibration using both complementary recursive prediction and adaptive Kalman filtering," in *Proc. ION GPS 2000*, Salt Lake City, UT, USA, Sept. 19–22 2001, pp. 1735–1740.

[5] Lei Fang, P.J. Antsaklis, L.A. Montestruque, M.B. McMickell, M. Lemmon, Yashan Sun, Hui Fang, I. Koutroulis, M. Haenggi, Min Xie, and Xiaojuan Xie, "Design of a Wireless Assisted Pedestrian Dead Reckoning System - The NavMote Experience," *IEEE Transactions on Instrumentation and Measurement*, vol. 54, no. 6, pp. 2342–2358, Dec. 2005.

[6] P. Bahl and V.N. Padmanabhan, "Radar: An In-Building RF-based User Location and Tracking System," in *Proc. IEEE INFOCOM 2000*, 2000, vol. 2, pp. 775–785.

[7] A. Kotanen, M. Hännikäinen, H. Leppäkoski, and T. Hämäläinen, "Experiments on Local Positioning with Bluetooth," in *Proc. ITCC 2003*. IEEE Computer Society, 2003, pp. 297–303.

[8] M.A. Youssef, A. Agrawala, and A. Udaya Shankar, "WLAN Location Determination via Clustering And Probability Distributions," in *Proc. IEEE PerCom 2003*, March 2003, pp. 143–150.

[9] M. A. Quddus, W. Y. Ochieng, and R. B. Noland, "Current map-matching algorithms for transport applications: State-of-the art and future research directions," *Transportation Research Part C*, vol. 15, no. 5, pp. 312–328, 2007.

[10] F. Evennou, F. Marx, and E. Novakov, "Map-aided Indoor Mobile Positioning System using Particle Filter," in *Proc. IEEE 2005 Wireless Communications and Networking Conference*, 2005, vol. 4, pp. 79–84.

[11] Hui Wang, H. Lenz, A. Szabo, J. Bamberger, and U.D. Hanebeck, "WLAN-Based Pedestrian Tracking Using Particle Filters and Low-Cost MEMS Sensors," in *Proc. WPNC'2007*, Hannover, Germany, 2007, pp. 1–7.

[12] Widyawan, M. Klepal, and S. Beauregard, "A Novel Backtracking Particle Filter for Pattern Matching Indoor Localization," in *MELT '08: Proceedings of the first ACM international workshop on Mobile entity localization and tracking in GPS-less environments*, New York, NY, USA, 2008, pp. 79–84.

[13] O. Woodman, and R. Harle, "RF-Based Initialisation for Inertial Pedestrian Tracking," in *Pervasive '09: Proc. the 7th International Conference on Pervasive Computing*, Nara, Japan, 2009, pp. 238–255, Springer-Verlag.

[14] R.G. Brown and P.Y.C. Hwang, *Introduction to Random Signals and Applied Kalman Filtering*, John Willey & Sons, Inc., 3rd ed. edition, 1997.

[15] R. G. Brown, "Integrated Navigation Systems and Kalman Filtering: A Perspective," *NAVIGATION, Journal of The Institute of Navigation*, vol. 19, no. 4, pp. 355–362, 1972.

[16] H. Qi and J. B. Moore, "Direct Kalman Filtering Approach for GPS/INS Integration," *IEEE Transactions on Aerospace and Electronic Systems*, vol. 38, no. 2, pp. 687–693, 2002.

[17] Yunchun Yang, J. Farrell, and M. Barth, "High-Accuracy, High-Frequency Differential Carrier Phase GPS Aided Low-Cost INS," in *Proc. of the IEEE PLANS*, San Diego, CA, USA, 2000, pp. 148–155.

[18] V. Gabaglio, "Centralised Kalman Filter for Augmented GPS Pedestrian Navigation," in *Proc. ION GPS 2001*, Salt Lake City, Utah, USA, 2001, pp. 312–318.

[19] K. Frank, B. Krach, N. Catterall, and P. Robertson, "Development and Evaluation of a Combined WLAN & Inertial Indoor Pedestrian Positioning System," in *Proc. ION GNSS 2009*, Savannah, Georgia, USA, 2009, pp. 538–546.

[20] H. Leppäkoski and J. Takala, "Analysis of complementary Kalman filter configurations for navigation systems," in *Proc. ENC-GNSS'07*, Geneva, Switzerland, May 29–31 2007, pp. 1365–1376.

[21] J.V. Candy, *Bayesian Signal Processing: Classical, Modern, and Particle Filtering Methods*, John Willey & Sons, Inc., 2009.

[22] J. Elwell, "Inertial Navigation for the Urban Warrior," in *Proc. SPIE Conference on Digitalization of the Battlespace IV*, Orlando, Florida, USA, Apr. 7–8 1999, pp. 196–204.

[23] P.D. Groves, *Principles of GNSS, Inertial, and Multisensor Integrated Navigation Systems*, Artech House, 2008.

[24] H. Leppäkoski, S. Tikkinen, and J. Takala, "Optimizing Radio Map for WLAN Fingerprinting," in *Proc. UPINLBS*, Kirkkonummi, Finland, Oct. 14–15 2010, pp. 1–8.

[25] T. Roos, P. Myllymäki, H. Tirri, P. Misikangas, and J. Sievänen, "A probabilistic approach to wlan user location estimation," *International Journal of Wireless Information Networks*, vol. 9, no. 3, pp. 155–164, July 2002.

[26] VTI Technologies, "SCC1300-D04 combined gyroscope and 3-axis accelerometer with digital SPI interfaces," rev. 1.0.3. Doc.Nr. 82 1131 00 A, Data sheet, 2010.